# Mechanical Stability and Porosity Analysis of Large-Pore SBA-15 Mesoporous Molecular Sieves by Mercury Porosimetry and Organics Adsorption

**ARTICLE** *in* LANGMUIR · SEPTEMBER 2002

Impact Factor: 4.46 · DOI: 10.1021/la025782j



**2 AUTHORS:**

Martin Hartmann
Friedrich-Alexander-University of Erlangen-N…
**196** PUBLICATIONS **6,395** CITATIONS
SEE PROFILE

Ajayan Vinu
University of Queensland
**324** PUBLICATIONS **9,496** CITATIONS
SEE PROFILE

# Mechanical Stability and Porosity Analysis of Large-Pore SBA-15 Mesoporous Molecular Sieves by Mercury Porosimetry and Organics Adsorption

Martin Hartmann* and A. Vinu

*Department of Chemistry, Chemical Technology, University of Kaiserslautern, PO Box 3049, D-67653 Kaiserslautern, Germany*

*Received March 27, 2002. In Final Form: June 11, 2002*

The mechanical stability of SBA-15 mesoporous silicas has been assessed using powder X-ray diffraction; nitrogen, benzene, and *n*-heptane adsorption; and mercury porosimetry. SBA-15 was found to possess rather low mechanical stability as compared to other mesoporous materials, viz., MCM-41 and MCM-48. These results can be explained by a simple mechanical model, which shows that SBA-15 has an unfavorable ratio between pore diameter and wall thickness. This ratio is more favorable for MCM-41 despite its smaller wall thickness. Our study confirmed that SBA-15 contains a significant amount of micropores in addition to the hexagonal arrangement of large mesopores. The amount (represented by the additional pore volume and surface area) of these complementary pores is tunable by variation of the synthesis temperature. It was shown that SBA-15 synthesized at temperatures higher than 120 °C contains almost no micropores. However, the pore size distribution of these materials is broader compared to materials synthesized at a lower temperature. The observed structural properties of the different SBA-15 materials are attributed to the changes in the degree of penetration of the poly(ethylene oxide) chains of the triblock copolymer within the silica walls of SBA-15.

## Introduction

The use of polymeric templates for the preparation of mesoporous silicas remarkably enhanced the opportunities in the synthesis of these materials. Polymeric templates are inexpensive and easy to recover and to recycle and allow expansion of the pore sizes for mesoporous molecular sieves well beyond 10 nm. Stucky and co-workers used triblock copolymers, star diblock copolymers, and oligomers for the synthesis of mesoporous ordered silicas such as SBA-11 and SBA-15.[1,2] Due to its robustness in terms of synthesis conditions, pore size adjustment, tailored particle morphology, and hydrothermal stability, the hexagonal phase SBA-15 is currently the most prominent member of the family of block copolymer templated materials. A wide range of applications in the field of adsorption, catalysis, and advanced materials is envisaged for this material. Applications such as heavy metal retardation[3] and sequestration and controlled release of proteins[4] have been developed by surface modification of SBA-15. AlSBA-15[5,6] and TiSBA-15[7,8] are interesting materials for catalysis. SBA-15 materials have also been employed as templates for Pt and Ag nanowires[9,10] and as advanced optical devices such as waveguides and mirrorless lasers.[11]

In light of the tremendous potential for different applications, the structural properties of SBA-15 have been carefully examined. In particular, the presence of micropores and their location has prompted several studies in recent years.[12−17] Low-temperature nitrogen adsorption isotherms are commonly used to evaluate the pore structure of mesoporous materials such as SBA-15. In comparison to the vast amount of nitrogen data, only little effort has been made to explore the potential of these materials in hydrocarbon adsorption.[18,19]

Moreover, mechanical stability is an important characteristic of an adsorbent or catalyst for most practical applications. Prior to adsorption and catalytic studies and IR or electric conductivity measurements, the fine powders obtained by hydrothermal synthesis are routinely compacted at high pressure into pellets. Crushing strength is a critical requirement to conserve the pore volume, surface area, and pore diameter of the ideal original parent material. Data on the mechanical strength of other

* To whom correspondence should be addressed. Phone: +49-631-205-3559. Fax: +49-631-205-4193. E-mail: hartmann@rhrk.uni-kl.de.

(1) Zhao, D.; Huo, Q.; Feng, J.; Chmelka, B. F.; Stucky, G. D. *J. Am. Chem. Soc.* **1998**, *120*, 6024.
(2) Zhao, D.; Feng, J.; Huo, Q.; Melosh, N.; Fredrickson, G. H.; Chmelka, B. F.; Stucky, G. D. *Science* **1998**, *279*, 548.
(3) Liu, A. M.; Hidajat, K.; Kawi, S.; Zhao, D. Y. *Chem. Commun.* **2000**, 1145.
(4) Han, Y. J.; Stucky, G. D.; Butler, A. *J. Am. Chem. Soc.* **1999**, *121*, 9897.
(5) Luan, Z. H.; Hartmann, M.; Zhao, D.; Zhou, W. Z.; Kevan, L. *Chem. Mater.* **1999**, *11*, 1621.
(6) Gedeon, A.; Lassoued, A.; Bonardet, J. L.; Fraissard, J. *Microporous Mesoporous Mater.* **2001**, *44*−*45*, 801.
(7) Luan, Z. H.; Maes, E. M.; van der Heide, P. A. W.; Zhao, D. Y.; Czernuszewicz, R. S.; Kevan, L. *Chem. Mater.* **1999**, *11*, 3680.
(8) Newalkar, B. L.; Olanrewaju, J.; Komarneni, S. *Chem. Mater.* **2001**, *13*, 552.
(9) Huang, M. H.; Choudrey, A.; Yang, P. D. *Chem. Commun.* **2000**, 1063.
(10) Ryoo, R.; Ko, C. H.; Kruk, M.; Antochshuk, V.; Jaroniec, M. *J. Phys. Chem. B* **2000**, *104*, 11465.
(11) Yang, P.; Wirnsberger, G.; Huang, H. C.; Cordero, S. R.; McGhee, M. D.; Scott, B.; Deng, T.; Whiteside, G. M.; Chmelka, B. F.; Buratto, S. K.; Stucky, G. D. *Science* **2000**, *287*, 465.
(12) Kruk, M.; Jaroniec, M.; Ko, C. H.; Ryoo, R. *Chem. Mater.* **2000**, *12*, 1961.
(13) Miyazawa, K.; Inagaki, S. *Chem. Commun.* **2000**, 2121.
(14) Imperor-Clerk, M.; Davidson, P.; Davidson, A. *J. Am. Chem. Soc.* **2000**, *122*, 11925.
(15) Matos, J. R.; Mercuri, L. P.; Kruk, M.; Jaroniec, M. *Chem. Mater.* **2001**, *13*, 1726.
(16) Ravikovitch, P. I.; Neimark, A. V. *J. Phys. Chem. B* **2001**, *105*, 6817.
(17) Galarneau, A.; Cambon, H.; Di Renzo, F.; Fajula, F. *Langmuir* **2001**, *17*, 8328.
(18) Hartmann, M.; Bischof, C. *Prepr.—Am. Chem. Soc., Div. Pet. Chem.* **2001**, *46*, 23.
(19) Newalkar, B. L.; Choudary, N. V.; Kumar, P.; Komarneni, S.; Bhat, T. S. G. *Chem. Mater.* **2002**, *14*, 304.

10.1021/la025782j CCC: $22.00 
Published on Web 09/17/2002

mesoporous materials, viz., MCM-41 and MCM-48, were published by several groups.[18,20−25] For these materials, it has been shown that the loss of pore volume takes place without a significant decrease of the pore diameter. It is, therefore, surmised that a fraction of the pores are completely destroyed while the rest of the material is unaffected by the compression.

In the present work, the mechanical stability of the large-pore mesoporous material SBA-15 is investigated by mercury porosimetry and by adsorption of organics such as benzene and *n*-heptane and compared to data from nitrogen adsorption measurements. The large difference found for the pore volume derived from adsorption of organics and from nitrogen adsorption confirms the presence of micropores in our samples. It has been found that the amount of micropores present is tunable by variation of the synthesis temperature between 100 and 150 °C. The porosity of these materials has been further characterized by mercury porosimetry and *n*-heptane adsorption in comparison to the nitrogen adsorption data, revealing that for samples synthesized at $T = 130$ °C almost no micropores are present. However, due to partial decomposition of the polymeric template the pore size distribution is considerably broadened for samples synthesized at $T = 130$ °C.

## Experimental Section

**Synthesis.** SBA-15 was synthesized using the amphiphilic triblock copolymer poly(ethylene glycol)-*block*-poly(propylene glycol)-*block*-poly(ethylene glycol) ($EO_{20}PO_{70}EO_{20}$; average molecular weight, 5800; Aldrich).[5] A typical synthesis was performed as follows: 4 g of the amphiphilic triblock copolymer was dispersed in 30 g of water and 120 g of a 2 M HCl solution and stirred for 5 h. Thereafter, 9.5 g of tetraethyl orthosilicate (TEOS) was added to the homogeneous solution under stirring. The resulting gel was aged at 40 °C for 24 h and finally heated to 100 °C for 24 h. In a second set of experiments, the gels were prepared as described above and crystallized at different temperatures between 100 and 150 °C. After synthesis, the obtained solids were calcined in flowing air at 540 °C to decompose the triblock copolymer.

**Characterization.** The X-ray powder diffraction patterns were recorded on a Siemens D5005 diffractometer using Cu Kα radiation. Thermogravimetric analysis (TGA) measurements were carried out under nitrogen in a high-resolution thermogravimetric analyzer (SETARAM Setsys 16MS) with a heating rate of 5 K/min. Nitrogen adsorption and desorption isotherms were measured at 77 K on a Quantachrome Autosorb 1 sorption analyzer. The specific surface area was obtained using the standard Brunauer−Emmett−Teller (BET) method, while the pore size distribution was calculated from the adsorption branch of the isotherm by employing the Barrett−Joyner−Halenda (BJH) formalism. To test the mechanical stability of SBA-15, the samples were compressed in a steel die of 24 mm diameter, using a hand-operated press, for 30 min. The different external pressures applied (52, 130, and 260 MPa) were calculated from the external force and the diameter of the die. Subsequently, the obtained disk was crushed and sieved to obtain pellets with a diameter of 0.25−0.35 nm, which were used for all further experiments. The benzene and *n*-heptane uptake was determined at 283 K using a SETARAM Setsys 16MS instrument equipped with a fixed-bed saturator. Static *n*-heptane adsorption isotherms were measured with a home-built volumetric adsorption apparatus at 286 K. Prior to the adsorption experiments, the samples were dehydrated at 393 K in a nitrogen flow ($V/t = 50$ cm$^3$ s$^{-1}$). The mercury porosimetry data were collected on a Micromeritics Autopore II 9220 instrument.

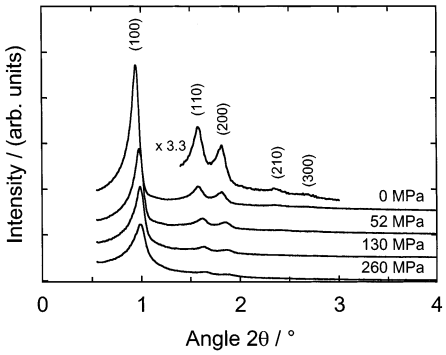


**Figure 1.** Powder X-ray diffraction patterns for SBA-15 mesoporous silicas compacted with different pressures.

## Results and Discussion

As-synthesized SBA-15 shows three reflections ((100), (200), and (110)) in the X-ray diffraction (XRD) patterns (not shown) corresponding to a unit cell parameter of 12.3 nm. After calcination, the XRD pattern exhibits five distinct peaks characteristic of a highly ordered hexagonal structure (Figure 1). The weight loss of the as-synthesized sample at temperatures between 353 and 823 K was determined by TGA to 26.3 wt %, which is in line with results from Kruk et al.[12] This weight loss can be attributed primarily to desorption and decomposition of the triblock copolymer and to a smaller extent to the release of water from condensation of the silanol groups in the silicate framework.[12]

Figure 1 exhibits the powder X-ray diffraction patterns of the compressed SBA-15-*p* (*p* denotes the pelletizing pressure) samples in comparison to the parent material SBA-15-0, which reveals five reflections ((100), (200), (110), (300), and (210)) indicative of a high-quality material with long-range ordering. The quality of the XRD patterns decreases with increasing pelletizing pressure up to 260 MPa (260 N mm$^{-2}$). The (100), (110), and (200) reflections are slightly shifted after compression, which indicates modest changes of the SBA-15 unit cell (Table 1). Moreover, the diffraction peaks broaden with increasing pelletizing pressure, which might suggest that larger grains are preferentially crushed while smaller grains survive the application of the external force. Such an interpretation is supported by the Scherrer equation which links the half-width of a diffraction line with the mean crystal size.

In Table 1, the results from evaluation of the nitrogen adsorption and desorption isotherms (Figure 2) using the BET and the BJH model, respectively, are summarized. With increasing pelletizing pressure, specific pore volume and specific surface area decrease, while the mean pore diameter calculated from the desorption branch of the nitrogen isotherms using the BJH model is virtually unaffected ($d_p = 6.7$ nm). The mean pore diameter calculated from the adsorption branch (which is predominantly used to characterize materials exhibiting $N_2$ isotherms with a large hysteresis loop) declines from 9.2 nm (SBA-15-0) to 8.0 nm (SBA-15-260). The pore size distribution (not shown) is broadened to the low pore diameter side, which indicates some pore deformation upon compression and, hence, a decrease of the mean pore

(20) Gusev, V. Y.; Feng, X.; Bu, Z.; Haller, G. L.; O'Brien, J. A. *J. Phys. Chem.* **1996**, *100*, 1985.
(21) Koyano, K. A.; Tatsumi, T.; Tanaka, Y.; Nakata, S. J. *J. Phys. Chem. B* **1997**, *101*, 9436.
(22) Tatsumi, T.; Koyano, K. A.; Tanaka, Y.; Nakata, S. *J. Porous Mater.* **1999**, *6*, 13.
(23) Hartmann, M.; Bischof, C. *J. Phys. Chem. B* **1999**, *103*, 6230.
(24) Desplantier-Giscard, D.; Collart, O.; Galarneau, A.; Van der Voort, P.; Di Renzo, F.; Fajula, F. In *Nanoporous Materials II*; Sayari, A., Jaroniec, M., Pinnavaia, T. J., Eds.; Studies in Surface Science and Catalysis Vol. 129; Elsevier: Amsterdam, 2000; pp 665−672.
(25) Springuel-Huet, M.-A.; Bonardet, J. L.; Gédéon, A.; Yue, Y.; Romannikov, V. N.; Fraissard, J. *Microporous Mesoporous Mater.* **2001**, *44*−*45*, 775.

**Table 1. Selected Structural Parameters of SBA-15 after Compression at Different Pressures**

| sample | pressure/MPa | $a_0$/nm | specific surface area/($m^2$ $g^{-1}$) | specific pore volume/($cm^3$ $g^{-1}$) | $V/V_0$ | $d_{p,Hg}$/nm | $d_{p,ads}$/nm | $d_{4V/A}$/nm |
|---|---|---|---|---|---|---|---|---|
| SBA-15-0 | 0 | 10.89 | 1130 | 1.61 | 1 | 8.2 | 9.2 | 5.69 |
| SBA-15-52 | 52 | 10.52 | 1020 | 1.40 | 0.86 | 8.0 | 8.6 | 5.49 |
| SBA-15-130 | 130 | 10.42 | 950 | 1.20 | 0.74 | 7.8 | 8.2 | 5.05 |
| SBA-15-260 | 260 | 10.39 | 880 | 0.96 | 0.59 | 7.0 | 8.0 | 4.35 |

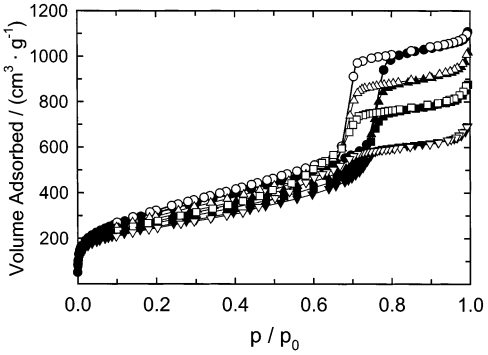


**Figure 2.** Nitrogen adsorption (closed symbols) and desorption (open symbols) isotherms at 77 K for SBA-15 compacted at different pressures: (○) 0 MPa, (△) 52 MPa, (□) 130 MPa, and (▽) 260 MPa.

diameter (Table 1) results. Application of the Gurvich method $d_{4V/A} = 4V_{mes}/A_{BET}$ allows a simple assessment of the pore diameter of a general mesoporous solid. However, in the case of SBA-15, the pore diameter is largely underestimated (Table 1). This is in line with previous studies stating that SBA-15 contains a secondary pore system with smaller pores in the micro- and/or mesopore regime.[10,18,26] Since high surface area/pore volume ratios are realized for narrow pores, the high surface areas calculated from our data also strongly indicate a secondary pore system with small mesopores or micropores.

To evaluate whether the secondary pore system is accessible for larger molecules, the uptake of benzene and *n*-heptane has been determined. In Figure 3a,b, the uptake curves of benzene and *n*-heptane at 283 K over the compressed SBA-15 materials are depicted in comparison to the unpressed parent material. The uptake curves are characterized by three distinct regions: The initial fast uptake is ascribed to the adsorption of the organic compound at the inner surface of the pores. Subsequently, a plateau is reached, at which the relative pressure $p/p_0$ increases until capillary condensation of the organic adsorptive in the mesopores of SBA-15 sets in. Together with the relative pressure ($p/p_0$, adjusted by the saturator temperature), the total uptake represents one point of the corresponding equilibrium adsorption isotherm. Therefore, the total uptake at $p/p_0 = 0.95$ can be used to calculate the total pore volume accessible to benzene and *n*-heptane by employing the Gurvich rule. The results of these calculations are summarized in Table 2. The pore volumes calculated from the *n*-heptane and benzene uptake are significantly lower (up to 50%) than those calculated from the nitrogen adsorption isotherms (Table 1). The calculated pore volumes $V$ and the relative pore volumes $V/V_0$ ($V_0$ is the pore volume of the unpressed parent material) are displayed in parts a and b of Figure 4, respectively. For benzene and *n*-heptane, the pore volume decreases linearly from 0.96 to 0.55 $cm^3$ $g^{-1}$ (43%), while the pore volume determined by nitrogen adsorption decreases by 0.65 $cm^3$ $g^{-1}$ from 1.61 to 0.96 $cm^3$ $g^{-1}$ (40%). In previous studies on MCM-41 and MCM-48, it was also found that the pore

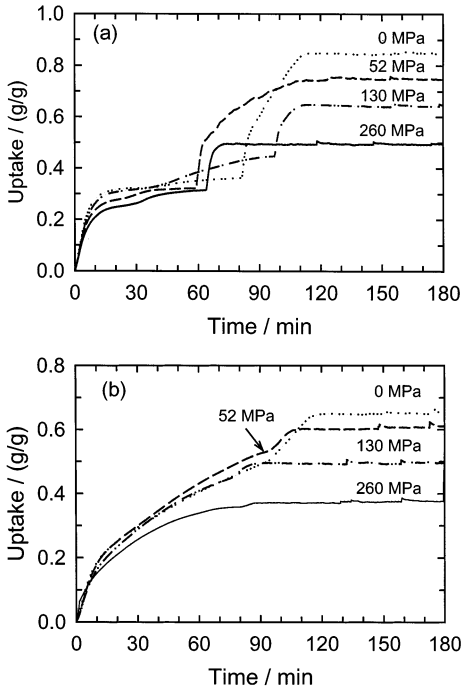


**Figure 3.** Uptake curves at 283 K of (a) benzene and (b) *n*-heptane for pelletized SBA-15.

volumes determined by adsorption of subcritical organic vapors are systematically lower (10−15%) than the ones calculated from nitrogen data.[23,27,28] This finding was mainly ascribed to the uncertainty of the density of the adsorbed phase which is taken as the density of the bulk liquid at the adsorption temperature (Gurvich rule). Furthermore, it was recently reported that the density of nitrogen adsorbed in the pores may be higher than that in the normal liquid,[28] which accounts for the differences obtained in the specific pore volume. In the considerably larger pores of SBA-15, however, the deviations of the adsorbed phase density from the bulk liquid density are presumably even smaller and, hence, are not able to explain the large differences (up to 50%) found in our study for SBA-15. On the other hand, some type IV isotherms do not obey the Gurvich rule. A possible explanation for this failure is that the particular adsorbent has micropores, giving molecular sieving in addition to its mesopore structure.[29] The rather large difference between the pore volume determined by nitrogen adsorption and those determined by adsorption of benzene and *n*-heptane, therefore, indicates that part of the SBA-15 pore system is not accessible for larger organics. It is very likely that part of the secondary pore system, which according to Kruk et al.[12] consists of small mesopores and micropores smaller than 1 nm, cannot be filled by benzene

(26) Lukens, W. W.; Schmidt-Winkel, P.; Zhao, D.; Feng, J.; Stucky, G. D. *Langmuir* **1999**, *15*, 5403.

(27) Nguyen, C.; Sonwane, C. G.; Bhatia, S. K.; Do, D. D. *Langmuir* **1998**, *14*, 4950.

(28) Ribeiro Carrott, M. M. J.; Candeias, A. J. E.; Carrott, P. J. M.; Ravikovitch, P. I.; Neimark, A. V.; Sequeira, A. D. *Microporous Mesoporous Mater.* **2001**, *47*, 323.

(29) Rouquerol, F.; Rouquerol, J.; Sing, K. *Adsorption by powders and porous solids*; Academic Press: San Diego, 1999; p 198.

**Table 2. Uptake of *n*-Heptane and Benzene ($p/p_0 = 0.95$) at 283 K and Calculated Pore Volumes Employing the Gurvich Rule**

| pressure/MPa | *n*-heptane uptake/(g/g) | pore volume/(cm$^3$ g$^{-1}$) | $V/V_0$ | benzene uptake/(g/g) | pore volume/(cm$^3$ g$^{-1}$) | $V/V_0$ |
|---|---|---|---|---|---|---|
| 0 | 0.661 | 0.97 | 1 | 0.848 | 0.96 | 1 |
| 52 | 0.602 | 0.88 | 0.91 | 0.747 | 0.84 | 0.88 |
| 130 | 0.497 | 0.72 | 0.75 | 0.645 | 0.73 | 0.76 |
| 260 | 0.377 | 0.55 | 0.57 | 0.493 | 0.56 | 0.58 |

or *n*-heptane. In a recent study, Jun et al.[30] showed that the structure of SBA-15 consists of a hexagonal arrangement of cylindrical mesopores with a diameter of 9 nm, which are randomly interconnected by micropores in the pore walls. This confirms that the secondary pore system has micropores and some of them might be too small to be accessible for the organics used in this study. In a control experiment, we determined the pore volume of large-pore MCM-41 ($d_p = 6$ nm) from the amount of nitrogen and *n*-heptane, respectively, adsorbed and found only a minor difference of ca. 5%.

The mechanical stability of SBA-15 is substantially smaller than those of MCM-41 and MCM-48.[23,24] For high-quality MCM-41 and MCM-48, the specific pore volume decreases only to 80% of its original value upon compression at 260 MPa,[24] while for SBA-15, the pore volume is diminished by about 40%. It is obvious that the mechanical stability of a hexagonal arrangement of pores increases with the wall thickness *w* but decreases with increasing pore diameter $d_p$. Therefore, the ratio $w/d_p$ is a good measure to compare the different hexagonal materials SBA-15 and MCM-41. For a typical MCM-41 ($w = 1.1$ nm, $d_p = 3.5$ nm),[24] $w/d_p$ equals 0.31, while for our SBA-15 ($w = a_0 - d_{p,ads} = 1.7$, $d_p = 9.2$) a $w/d_p$ of 0.18 results. From theoretical considerations, it is therefore expected that the mechanical stability of high-quality SBA-15 is lower than that of high-quality MCM-41, which is indeed confirmed in the present study. In agreement with previous studies on MCM-41[24,31] and MCM-48,[23] the loss in pore volume is accompanied only by a minor decrease in pore size. The decrease in pore volume is therefore mainly a consequence of the irreversible destruction under external stress (pressure) of the SBA-15 pore system, which is no longer accessible for larger molecules such as benzene and *n*-heptane or even nitrogen. Such a model is supported by the decrease of the relative pore volume $V/V_0$ (Figure 4b), which is independent from the molecules adsorbed. The observed almost linear decrease of the relative pore volume is unexpected even under uniform compression but might be explained in terms of successive compression of grains, where the stress is applied in the plane of the hexagonal section. With increasing pressure, the solid responds by successive crushing of planes of hexagonal cells until the stress is transmitted efficiently through the partly densified material. Further crushing of cells requires further increase of strain (viz., pelletizing pressure).

Mercury porosimetry is largely used to evaluate the porosity of industrial catalysts and other porous materials. Due to the high pressure needed to fill small pores, this method is at present limited to pores with $d_p > 4$ nm, which renders Hg porosimetry a useful characterization technique for our SBA-15 materials. In Figure 5, data for SBA-15 materials pressed at different pelletizing pressures are displayed. The pore diameter for SBA-15-0 is determined to be 8.2 nm in close agreement with the results from BJH analysis of the adsorption branch of the

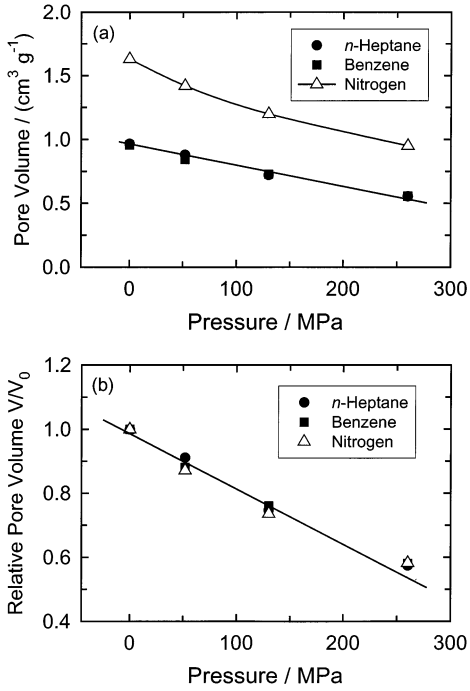


**Figure 4.** Comparison of (a) pore volumes and (b) relative pore volumes $V/V_0$ of pelletized SBA-15 calculated from the adsorption of nitrogen, benzene, and *n*-heptane.

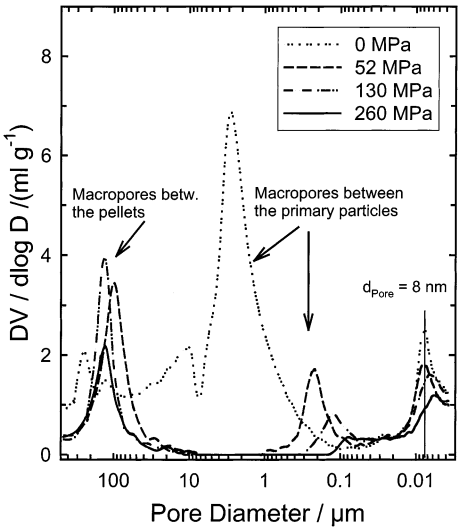


**Figure 5.** Pore size evaluation by mercury porosimetry of SBA-15 samples compacted at different pressures.

respective nitrogen isotherm. The pore diameter decreases slightly with increasing pelletizing pressure, and the pore size distribution broadens. The results obtained by mercury porosimetry are in qualitative agreement with the analysis of the nitrogen adsorption data, which confirms that the adsorption branch has to be analyzed to obtain reliable pore size distribution data for large-pore materials.

The second maximum around 2 $\mu$m (Figure 5) is ascribed to the filling of the void spaces (macropores) between the

(30) Jun, S.; Joo, S. H.; Ryoo, R.; Kruk, M.; Jaroniec, M.; Liu, Z., Ohsuna, T.; Terasaki, O. *J. Am. Chem. Soc.* **2000**, *122*, 10712.

(31) Galarneau, A.; Desplantier-Giscard, D.; Di Renzo, F.; Fajula, F. *Catal. Today* **2001**, *68*, 191.

**Table 3. Characterization Data for SBA-15 Synthesized at Different Temperatures**

| synthesis temperature/°C | unit cell size $a_0$/nm | specific surface area $A_{BET}$/($m^2/g^{-1}$) | specific pore volume $V_p$/($cm^3/g^{-1}$) | pore diameter/nm | $(4V_p/A_{BET})$/nm |
|---|---|---|---|---|---|
| 100 | 10.22 | 1100 | 1.60 | 9.0 | 5.1 |
| 110 | 10.52 | 1036 | 1.30 | 8.9 | 5.0 |
| 120 | 10.52 | 883 | 1.27 | 9.2 | 5.8 |
| 130 | 10.54 | 546 | 1.19 | 8.7 | 8.7 |
| 140 | 10.58 | 427 | 1.13 | 10.6 | 10.6 |
| 150 | 10.83 | 393 | 1.10 | 11.2 | 11.2 |

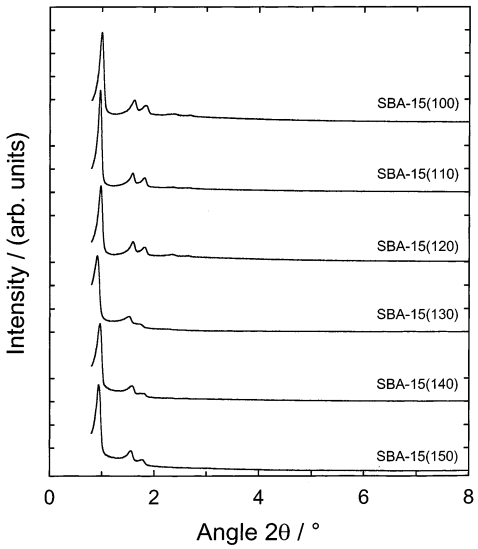


**Figure 6.** Powder X-ray diffraction patterns of SBA-15 materials synthesized at different temperatures.

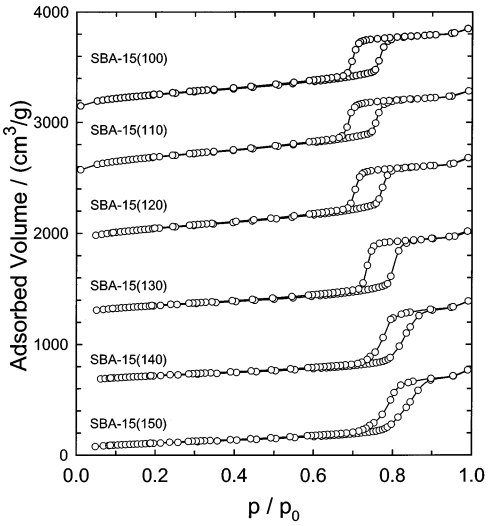


**Figure 7.** Nitrogen adsorption and desorption isotherms at 77 K of SBA-15 mesoporous silicas. The adsorption isotherms are shifted by 800 $cm^3\ g^{-1}$ relative to each other.

primary particles. The study of the intergranular porosity shows that the particles are getting closer under pressure. Therefore, the size and the number of these pores decrease with increasing pelletizing pressure. For the pellets, a new maximum at ca. 100 $\mu$m is observed which represents the toroidal void space of a collection of solid particles.[32] The size of these macropores mainly depends on the pellet size and, hence, is independent of the pelletizing pressure.

The adsorption and mercury porosimetry data reveal that the decrease in adsorption capacity is accompanied only by a minor decrease in pore size. Consequently, the mechanical degradation can be explained only by an irreversible destruction of the SBA-15 particles by zones. At a certain pressure, some zones remain intact while some others are totally crushed. With increasing pelletizing pressure, the fraction of crushed particles also increases and, hence, the material is getting denser and denser. To understand the evolution of porosity of hexagonal silica materials, calculation methods used for macroscopic cellular solids have been applied.[31]

To further evaluate the adsorption properties, we have synthesized SBA-15 samples at different temperatures between 100 and 150 °C (Table 3). In Figure 6, the XRD powder patterns of SBA-15 materials synthesized at different temperatures are displayed. The XRD patterns are very well-defined and characteristic of well-ordered hexagonal materials. The respective nitrogen adsorption isotherms (Figure 7) are of type IV and exhibit hysteresis of type H1 according to the IUPAC classification, which is typical for materials with constant cross section. The pore-filling step in the adsorption ($p/p_0 > 0.8$) and desorption isotherms is sharp (for the samples synthesized below 130 °C) as expected for a large-pore material with a narrow pore size distribution. The data obtained from

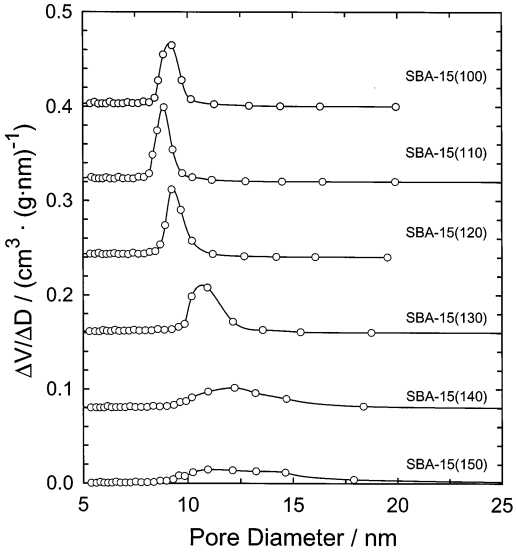


**Figure 8.** Pore size distributions for the SBA-15 mesoporous silicas.

examination of the nitrogen isotherms are visualized in Figures 8 and 9. The mean pore diameter increases with increasing synthesis temperature (Figure 8). For the samples synthesized at $T \geq 130$ °C, the pore size distribution broadens considerably. Figure 9 shows that specific pore volume and surface area decrease with increasing synthesis temperature. The specific pore volume decreases from 1.6 $cm^3\ g^{-1}$ for SBA-15(100) to 1.19 $cm^3\ g^{-1}$ for SBA-15(150), while the surface area decreases from 1130 to 393 $m^2\ g^{-1}$ for the same samples. The pore diameter of SBA-15(100) calculated from the nitrogen adsorption isotherm using the BJH method is confirmed by Hg porosimetry (Figure 10), which shows mesopores with a diameter of ca. 8 nm. The mean pore diameter

(32) Mayer, R.; Stowe, R. A. *J. Phys. Chem.* **1966**, *70*, 3867.

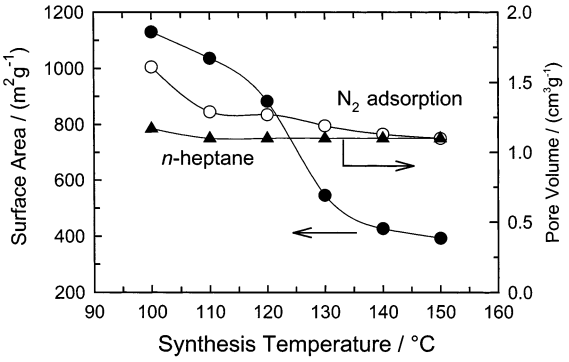


**Figure 9.** Evolution of surface area (●) and pore volume determined by nitrogen (○) and *n*-heptane (▲) adsorption as a function of the synthesis temperature.

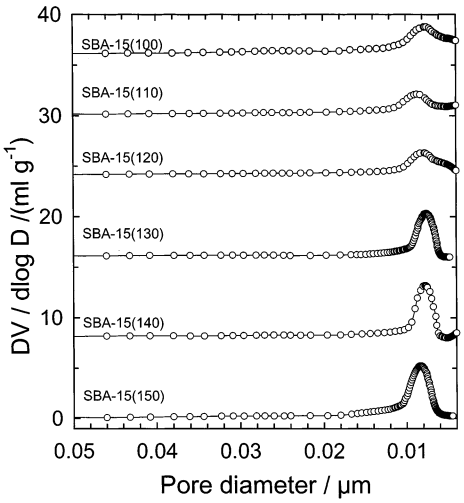


**Figure 10.** Pore size distribution obtained from mercury porosimetry for SBA-15 samples synthesized at different temperatures.

increases steadily with increasing synthesis temperature up to 10.8 nm for the sample synthesized at 150 °C, which is in close agreement with the nitrogen adsorption data (cf. Figure 8). Furthermore, also broadening of the pore size distribution with increasing synthesis temperature is observed.

For a material containing only cylindrical pores, the surface area is related to pore volume and pore diameter by the simple equation $A = 4V_p/d_p$. Consequently, for a sample containing mesopores with a diameter of 10 nm and having a specific pore volume of 1.6 $cm^3\,g^{-1}$, the surface area may not exceed 640 $m^2\,g^{-1}$. It is therefore clear from these simple geometrical calculations that the samples synthesized below 130 °C should contain a secondary pore system with micropores or small mesopores to explain the large surface area obtained. The existence of such a secondary pore system in SBA-15 samples prepared under certain conditions has also been observed in independent studies.[10,12,14,16,17] To probe the accessibility of the mesopore system for larger molecules, we also recorded the *n*-heptane adsorption isotherms. Figure 11 shows adsorption isotherms of *n*-heptane on SBA-15 samples synthesized at different temperatures. All isotherms are of type IV of the IUPAC classification and exhibit a H1 hysteresis loop. (The desorption points have been omitted for clarity.) The pressure needed to start capillary condensation increases slightly with increasing synthesis temperature, giving further evidence for the increase of the pore diameter. The pronounced difference in the low-pressure region between the samples synthesized at temperatures below

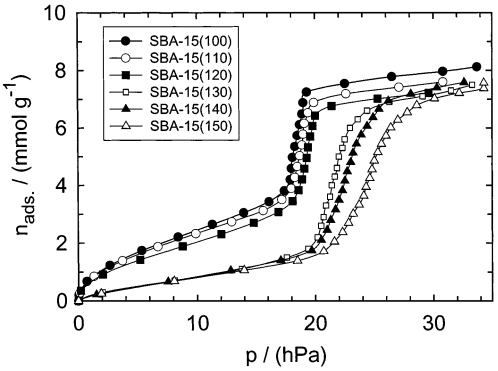


**Figure 11.** *n*-Heptane adsorption isotherms at 287 K of SBA-15 mesoporous silicas.

130 °C and those prepared above this temperature can clearly be ascribed to the presence of smaller pores in the micropore regime. The specific pore volumes calculated from the *n*-heptane isotherms using the Gurvich rule are also plotted in Figure 9. With increasing synthesis temperature of the SBA-15 samples, the difference between the specific pore volumes calculated from the nitrogen and *n*-heptane adsorption data declines. Finally, for SBA-15(140), the two values are almost identical and, hence, only the primary mesopores with a diameter of ca. 11 nm are present. In that particular case, also the geometrical equation $d_p = 4V_p/A$ is fulfilled, which also confirms the absence of the secondary pore system.

The formation of micropores (connecting the hexagonally arranged mesopores) in the SBA-15 synthesis at temperatures below 130 °C might be explained by the occurrence of some interactions between micelles of the triblock copolymer surfactant through ethylene oxide headgroups.[17] It is surmised that poly(ethylene oxide) (PEO) chains of the micelle sharing their hydration sphere are responsible for the formation of the micropores. With increasing synthesis temperature, the PEO chains are partially dehydrated and, hence, the volume of the hydrophilic part decreases (this probably results in the formation of smaller micropores). The partial dehydration of the PEO chain at higher temperatures facilitates sharing of the hydration sphere of different micelles, which probably has two consequences: The outer hydrophilic layer of the polymer chain decreases, and hence the micelle size increases. Second, the interactions between the micelles through their PEO groups decrease, viz., the PEO chains are closer to the PPO part of the same micelle, which results in the observed decrease of the microporosity. The triblock copolymer starts to decompose around 130 °C,[17] which most likely results in a significant variation in polymer size and, hence, size of the micelles formed. Moreover, the above-described mechanism of increase of the micelle size is still operative, and the micelles still grow despite a partial decomposition of the triblock copolymer. These variations in micelle size are reflected in a substantial broadening of the pore size distribution of the materials synthesized at temperatures above 130 °C.

A detailed account of the influence of the synthesis temperature on the porosity has been published recently by Galarneau et al.,[17] who exclusively analyzed nitrogen adsorption data. We note that our results complement their data and fully support their conclusions. However, a close inspection reveals minor differences; for example, the specific pore volume declines with synthesis temperature in our study, while Galarneau et al. report an increase in $V_p$. Our samples exhibit a higher initial

microporosity, so that the increase in pore volume due to the increased pore diameter is overcompensated by the loss of micropore volume. Therefore, we have to point out that every SBA-15 sample is unique and, consequently, the adsorption properties differ widely. In particular, pore diameter and wall thickness as well as the presence of microporosity influence the mechanical stability and also the properties of SBA-15 molecular sieves in catalysis and adsorption. A detailed knowledge of the synthesis strategies resulting in materials with predefined properties allows tailoring of adsorbents and catalysts.

## Conclusions

In the present study, the mechanical stability and the porosity of SBA-15 samples has been analyzed by adsorption experiments and mercury porosimetry. The adsorption of benzene and *n*-heptane confirms a considerable alteration of the SBA-15 pore structure by applying an external force. Up to a pressure of 260 MPa, the adsorption capacity calculated from the adsorption of both nitrogen and subcritical organics indicates a 40% decrease of the specific pore volume. The reduced adsorption capacity is assumed to be due to an irreversible destruction of a fraction of the pores, while the rest of the material is unaffected by the compression. The mechanical stability of SBA-15 is smaller than that of MCM-41 due to an unfavorable wall thickness/unit cell size ratio.

Besides the primary pore system of hexagonally arranged pores with a diameter of 9 nm, further evidence is found for a secondary pore system with small micropores, which are partially not accessible for larger organics, viz., benzene and *n*-heptane. Selective investigation of the mesopore system reveals that up to 50% of specific surface area and pore volume are due to microporosity. This fraction can be reduced to zero by raising the synthesis temperature to 130 °C.

Mercury porosimetry has been used for the first time for the characterization of mesoporous SBA-15 materials. It has been shown that this method is useful for large-pore mesoporous molecular sieves, allowing a reliable determination of pore size and intergranular porosity.

**Acknowledgment.** Financial support of this work by Deutsche Forschungsgemeinschaft (Ha2527/4-1) and Fonds der Chemischen Industrie is gratefully acknowledged. M.H. thanks Professor S. Ernst for generous support.

LA025782J